EARTH'S CRYOSPHERE
SCIENTIFIC JOURNAL

Earth's Cryosphere, 2022, vol. XXVI, No. 5, pp. 48–60

SNOW COVER AND GLACIERS

SUPERIMPOSED ICE ON THE BELLINGSHAUSEN DOME, KING GEORGE ISLAND, ANTARCTICA

B.R. Mavlyudov

Glaciology Department, Institute of Geography, Russian Academy of Sciences, Staromonetnyj per. 29, Moscow, 119017 Russia

E-mail: bulatrm@bk.ru

Conditions of the origin, existence, and melting of the superimposed ice are considered for the Bellingshausen Ice Dome on Fildes Peninsula of King George (Waterloo) Island near Antarctic Peninsula. Every year, accumulation of superimposed ice on the ice dome reaches about 15 cm. In years with positive mass balance on the ice dome, the thickness of superimposed ice increases. The maximum measured thickness of perennial superimposed ice on the ice dome is about 145–150 cm reaching 300 cm in some places. Significance of the superimposed ice in the ice mass balance of the Bellingshausen Ice Dome in different years during the observation period from 2007 to 2021 is estimated. It is argued that regime of field observations are necessary for finding seasonal boundary of the superimposed ice as equilibrium line altitude.

Keywords: *Bellingshausen Ice Dome, Fildes Peninsula, ice mass balance, superimposed ice.*

Recommended citation: Mavlyudov B.R., 2022. Superimposed ice on the Bellingshausen Dome, King George Island, Antarctica. *Earth's Cryosphere* **26** (5), 48–60.

INTRODUCTION

The author, following [*Cuffey, Paterson, 2010; Congley et al., 2011*], considers superimposed ice (SI) to be a continuous ice layer forming in the lower part of the snow or snow–firn thickness at the boundary with the glacier ice. In Russian literature, an analogous layer of ice is called infiltration-congelation ice [*Kotlyakov, 1984*], or also superimposed ice [*Ushnurtsev et al., 1995*]. The SI thickness increases until the entire cold store in the underlying ice is used [*Cuffey, Paterson, 2010*]. In the annual snow layer on the glacier, all the formed SI melts together with the snow. In the long-term snow–firn thickness, the SI is preserved and is an element of internal feeding [*Bazhev, 1973, 1980*].

The role of SI in the life of glacier is discussed in numerous publications [*Baird, 1952; Fujita et al., 1996; Wadham, Nuttal, 2002*]. Almost all researchers believe that SI plays an important and sometimes a decisive role in glacier ice mass balance in Polar regions [*Wright et al., 2007*] and regions with continental climate [*Koreisha, 1991*]; in other regions, the role of SI is considered insignificant [*Cuffey, Paterson, 2010*].

For the glaciers of King George Island, a widespread distribution of SI is typical on the surface of ice domes after the snow melting; in particular years, SI cover vast areas. However, this phenomenon is rarely mentioned in publications on this region; the description and mention of SI on King George Island can be found in [*Gonera, Rachlewicz, 1997; Rachlewicz, 1999*]; on Signy Island (the South Orkney Islands) in [*Gardiner et al., 1998*].

In general, SI remains insufficiently studied, especially in Antarctic regions. The present work discusses SI formation on King George Island with a focus on the Fildes Peninsula and the Bellingshausen Dome located on this peninsula, where field work was conducted during 2007–2012 and 2014–2021 within the framework of seasonal studies of the Russian Atarctic Expedition. In addition to understanding the specificity of the formation and existence of SI, an attempt was made to determine its role in the ice dome mass balance.

MATERIALS AND METHODS

Study area

Field study of SI was conducted on the Fildes Peninsula (62° S) in the southwestern part of King George (Waterloo) Island in the South Shetland Islands Archipelago, near the northern end of the Antarctic Peninsula (Fig. 1).

The Fildes Peninsula is 3 km wide and 10 km long; the Bellingshausen Dome is found in its northeastern part (Fig. 2*a*). The size of the dome is 3.3 × 4.5 km, the height is 250 m asl, and its surface area is approximately 8.9 km^2. The Bellingshau-

sen Dome continuously adjoins to other, larger ice domes of the island, which is on 95% covered by ice. More detailed information about the structure of the Bellingshausen Dome can be found in [*Mavlyudov, 2016*].

Climate

The King George (Waterloo) Island is one of the warmest regions of Antarctica. The climate of King George is maritime, with mild winters and cool summers, because of the proximity of the Southern Ocean. In summer, west to north winds dominate and bring relatively warm air masses from the Pacific Ocean; in winter, east to south winds carry cold masses from the Antarctic continent. However, during the winter, northwest bringing not only warm air but also liquid precipitation can intrude. A period with above-zero air temperatures mainly lasts from December to March. The mean annual air temperature, according to the Bellingshausen weather station [*www.aari.aq*], is –2.3°C, the mean winter temperature (April–November) is –3.9°C, and the mean summer temperature (December–March) is 0.97°C. The mean annual precipitation is 697 mm with approximately 239 mm in summer (mostly as rain) and 458 mm in winter (mostly as snow).

Research methods

The study of SI on Fildes Peninsula and on the Bellingshausen Dome was conducted simultaneously with mass balance research. Superimposed ice was studied: (1) in the base of pits excavated for measuring snow on the ice dome at the end of November – beginning of December (if SI formation had already started by that time) and during summer seasons in the period of presence of a snow cover at stakes R1, R4, R8, R12, BN, FN, and IN; (2) during the period of snow cover melting, when the SI was entirely exposed (Figs. 2*b*, *c*, *e*); and (3) during the period of SI melting, when the melting crust is formed on its surface (Fig. 2*f*). The melting crust is a highly friable 5- to 10-cm thick top layer in the glacier's ablation area, which appears as a result of direct penetration of solar radiation into the ice, which induces ice melting in the upper layer [*Kotlaykov, 1984; Mavlyudov, 2008*]. The SI thickness was measured in boreholes (Fig. 2*d*) drilled by a ring drill of 10 cm in diameter at different times along the edge of the exposed SI (Table 1). The lower boundary of annual SI in boreholes was a layer of volcanic ash particles, which at the end of the ablation season usually appear at the surface of glacial ice.

The SI thickness was also measured on the walls of fresh crevasses and near 29 ablation stakes installed across different slopes of the ice dome (Fig. 1). The density of the SI and melting crust over it were determined by weighing method.

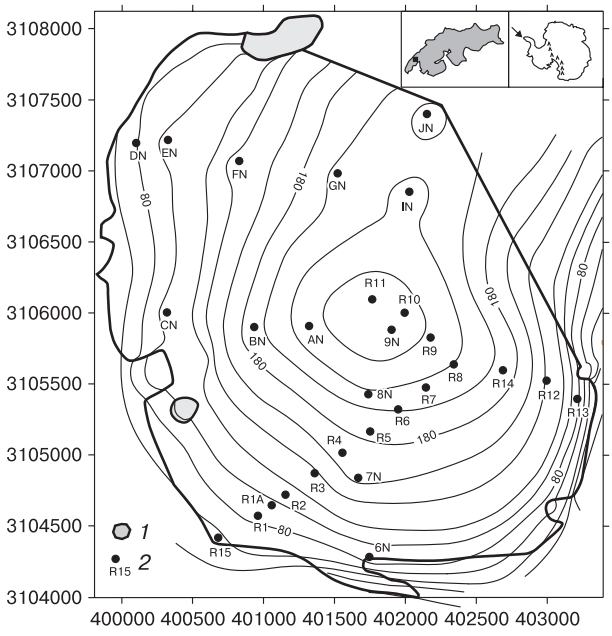

Fig. 1. Location of Bellingshausen Ice Dome and ablation stakes on it.

1 – nunataks, *2* – ablation stakes and their numbers. Inset maps show the position of King George Island (*arrow*) near Antarctic Peninsula and the Bellingshausen Ice Dome (*black square*) on King George Island (UTM coordinate system, zone 21).

RESULTS

Identified conditions of superimposed ice formation

The formation of SI depends on the structure, thickness and temperature of the snow thickness, store of cold accumulated in the underlying ice over the winter, and on the surface structure of glacial ice [*Kotlyakov, 1984*]. Study of the snow cover structure before the beginning of melting demonstrated that it consists of snow layers of varying granularity and density, as well as numerous ice interlayers. Ice layers in the snow thickness can be of two types. The first is ice crust forming upon rainfall onto a cold surface of snow. Ice crusts are usually continuous, and their thickness does not exceed 1–3 mm. Thinner ice crusts are formed upon periods of abrupt warming without liquid precipitation (radiation crusts). The second is ice interlayer forming during the concretion of water vapor onto the surface of the snow during strong winds (most often, northern and northwestern) under conditions of high air humidity (fog) and near-freezing temperature. In this case, single ice aggregates of about 2 cm wide, 2–4 cm long and approximately 1 cm thick grow on the surface of the snow cover. These aggregates are inclined at 10°–20° to the surface of the snow and are oriented against air flows. In such layers, ice aggregates are not interconnected.

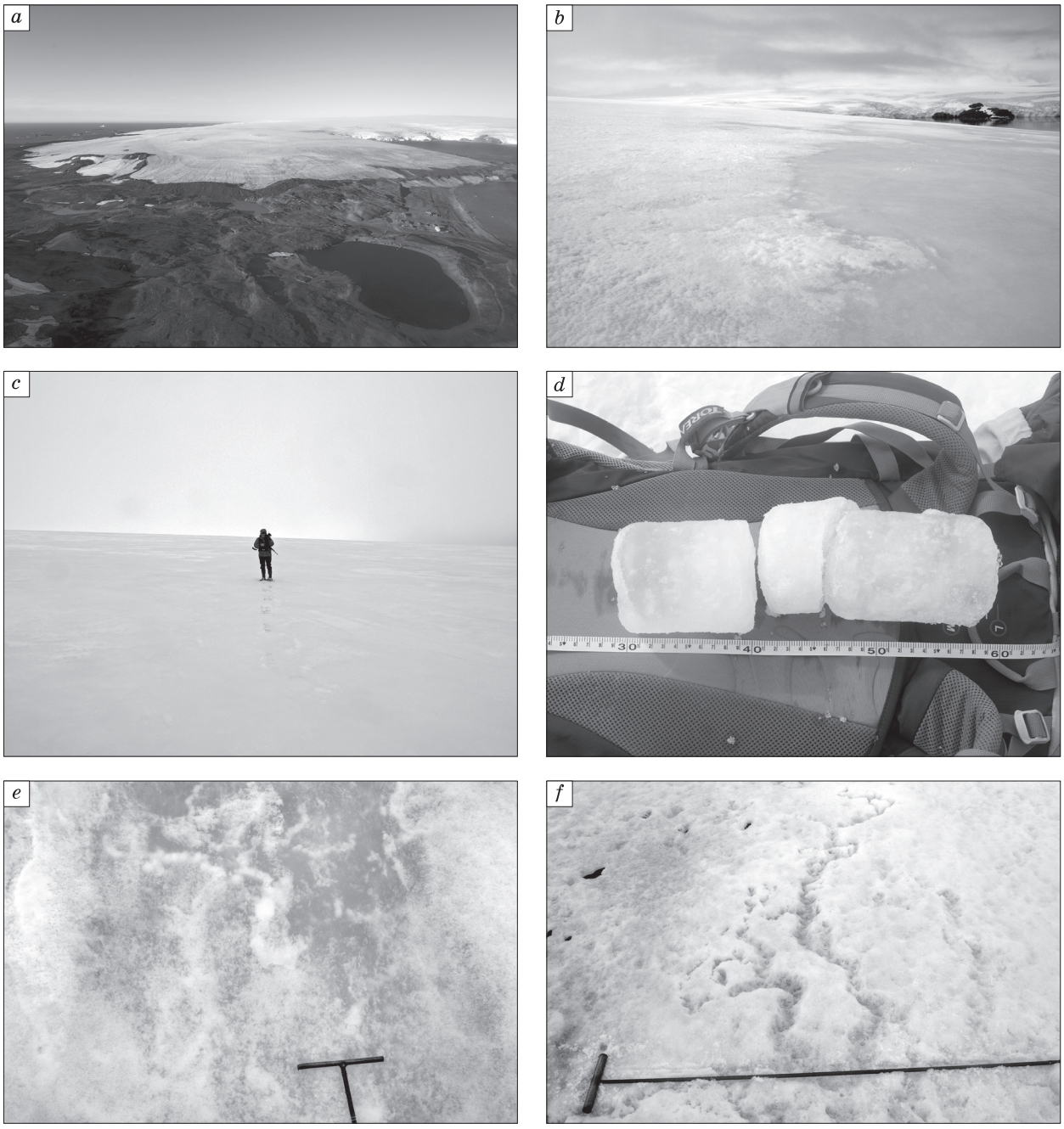

Fig. 2. Bellingshausen Ice Dome: (*a*) view from the southeast from a helicopter (March 7, 2020), (*b*) boundary between snow and exposed SI on southern slope of the dome, (*c*) SI field on southern slope of the dome (December 31, 2019), (*d*) core of the long-term SI, (*e*) surface of the exposed SI with translucent inner channels, and (*f*) melting crust with melted out inner channels on the surface of exposed SI.

The overall thickness of the layers with ice aggregates usually does not exceed 2–3 cm.

At the beginning of the warm season, meltwater seeps through snow to ice interlayers, beginning to increase the thickness of ice crust and bind together ice aggregates. However, the heat released during the freezing of meltwater on ice interlayers most often does not allow a significant increase in their thickness. As a result, water finds a way through the ice crust or between ice aggregates and infiltrates into deeper layers. However, in some cases, meltwater makes ice interlayers impermeable. In this case, ice begins to grow over these ice interlayers and isolates layers and lenses of snow or firn within the ice thickness.

Table 1. **Characteristics of superimposed ice on the Bellingshausen Ice Dome in different years**

Year	Average SI thickness for the dome, cm	Range of SI thickness variation, cm	Average SI thickness according to stake measurements, cm w.e.	SI melting, cm w.e.	SI share in B_w according to stake measurements, %	SI share in B_s according to stake measurements, %
2007/08	19.9 (214)	1–28	18.1	8.8	28.3	12.0
2008/09	16.0 (107)	7–43	14.3	9.3	26.9	7.4
2009/10	15.6 (76)	4–27	14.4	0.7	18.3	1.6
2010/11	38.9 (53)	4–52	13.4	8.7	21.4	17.2
2011/12	30.3 (20)	10–69	16.1	14.4	28.5	12.6
2012/13				0		0
2013/14				0		0
2014/15	41.7 (29)	5–54	12.4	0.9	23.0	1.6
2015/16	25.7 (60)	8–56	16.4	3.1	27.8	5.5
2016/17	30.7 (36)	6–175	14.9	16.5	28.1	17.6
2017/18	14.6 (34)	5–150	14.4	19.0	24.4	19.5
2018/19	13.6 (40)	5–35	12.9	4.7	20.7	9.1
2019/20	67.1 (64)	3–300	11.8	31.6	23.0	18.1
2020/21	13.8 (122)	5–106	10.9	10.9	13.4	10.9

Note: Number of measurements is indicated in parentheses. B_w is the winter mass balance, and B_s is the summer mass balance. Bold face in the first column indicates years with positive mass balance.

A portion of ice in the snow thickness on the ice dome differed significantly from year to year and from point to point because it depended on the thickness and structure of the snow, slope orientation, and weather conditions during previous periods. During all years of observation, at the end of the season of accumulation, at maximum snow accumulation, the amount of ice (by water content) within the seasonal snow thickness ranged from 12 to 60% given the average snow thickness of 0.4–0.5 g/cm^3. During the season of ablation, the overall amount of ice in the seasonal snow initially increased and then decreased.

Measured snow temperatures at the bottom part of the snow thickness at the end of the season of accumulation on the Bellingshausen Dome in different years varied from –3 to –5°C. Low snow temperature contributed to freezing of meltwater seeping from the surface of the snow and moistening the snow thickness with the growth snow grains as well as to the increase in the thickness of ice interlayers. The SI formation in the lower part of the snow–firn thickness took place primarily during its moistening by meltwater. In some cases, this process could begin earlier, if meltwater flowed or seeped through down the slope under the snow thickness from higher positions with a thinner snow, where it melted first, how it happened, for example, on the slope below stake R4.

Measurements in pits showed that the average mineralization of seasonal snow in the upper part of the ice dome was approximately 70 mg/L. During water flowing down the ice slope, its partial freezing (during SI formation) took place, which led to increasing concentration of salts in the water flowing over the ice. At the beginning of the ablation season, water mineralization reaching 1000 mg/L) was measured several times in the pits in the lower part of the snow thickness. This indicates that the water made quite a long way under the snow. The recorded mineralization of the SI itself was 20–30 mg/L. The measured velocity of water flow under the 1-m-thick snow cover on a slope of about 10° reached approximately 80 m/day. If the rate of water flow down the dome's slopes is considered as a constant, meltwater can flow down from the top of the dome to its lower part in 18–19 days. This rate increases as the steepness of the slope increases and the snow thickness decreases. The latter leads to the growth of the thickness of the moistened layer in the lower part of the snow thickness which achieves a maximum in a strip of water-saturated snow ("snow bog") at the boundary of the snow cover and the exposed SI. Upon the emergence of a thick layer of wet snow, the formation of SI slows down and then ceases. According to the author's estimates, the duration of SI growth on the dome during the spring is 1–1.5 months and depends on the air temperature and the activity of spring snowmelt. At the same time, the growth of the SI layer occurs on the whole snow-covered surface of the ice dome. Apparently, an exception is the areas of the ice dome, where the long-term snow–firn thickness is maximal, i.e., where it exceeds 3 m, so that SI forms within this thickness and meltwater runoff during the ablation season is minimal.

It was determined that snow disappears first in the areas with the minimum snow thickness in the middle of the southern (near stake R4) and north-

western (near stakes EN and FN) slopes and at the lower part of the dome (if there is no windblown snow pack there). An area of melted snow appeared in the snow field and began to grow in all directions increasing the area of the exposed SI layer. The exposed SI begins to melt, and a layer of melting crust – a loose mass of weakly cemented ice grains of 1–2 mm in diameter – forms on it. After the SI melting, glacier ice is exposed to the surface, and the area of SI encircles exposed glacier ice. Subsequently, the area of exposed glacier ice also begins to increase. Meltwater channels form in the exposed field of glacier ice and are drained down the slope, first into the strip of SI, then also into the area of snow. In the case of active melting and considerable meltwater discharge through these channels, slush flows can form in the snow field. Getting toward the lower side of glacier ice, meltwater can sometimes penetrate under the edge of the partially melted SI and further flow beneath the SI at some distance. However, as the SI layer is frozen to the glacier ice at the contact with the snow field, meltwater flow under it becomes impossible. As a result, weakened areas of the SI layer appear in this zone, where meltwater discharge to the surface takes place in the form of small fountains giving the birth to surface water streams. Often, on the exposed surface of the SI layer on the dome, currently active and former fountains can be identified by the presence of dark spots of volcanic ash carried out by the meltwater streams onto the surface of the whitish SI. Volcanic ash is present in the form of interlayers within the glacier ice and is mainly derived from volcanic eruptions on Deception Island of the same archipelago 120 km to the west-southwest [*Jiankang et al., 1999*].

If the long-term snow–firn layer exceeds 2 m, as recorded near stakes R6–R9, then SI can also form on the surface of one of the ice interlayers near the bottom of the snow thickness at the end of the ablation season. Most often, this was observed at a distance of 0.5–0.8 m from the surface of the glacier ice, so that firn layer sealed from the top by SI was preserved. In 2016, the author measured the thickness of one of such suspended SI layers in the pit near stake R6; it equaled 25 cm and was formed over the course of 1.5 years. Subsequently, while the snow cover was preserved, the thickness of this SI layer increased. In this case, a new SI layer formed within the firn thickness, under which the layer of sealed firn was preserved. At the end of the 2018/19 summer season, the thickness of the suspended SI layer reached 70 cm. An analogous phenomenon was also noted at other measurement stakes in the upper part of the ice dome with a sharp decrease in the snow–firn thickness measured weekly using a metal probe during the ablation season.

In autumn, SI formation is favored by the conditions in the thin lower part of the snow cover. A new SI layer is formed, the thickness of which decreases in the direction of increasing snow thickness. A layer of autumn SI can be preserved until the next ablation season or melt together with the snow during the next summer warming.

At the end of the ablation season, the surface of the glacier ice becomes uneven, very dissected, cut by numerous channels deepened into the ice and forming along former ice cracks and other defects. Numerous recesses and rises of 10–15 cm in amplitude are typical for the ice surface during this time, as well as cryoconite holes of different sizes. The formation of SI in the autumn and, to a larger extent, in the spring leads to leveling of the ice surface. Consequently, during simultaneous snow melting in separate areas of the ice dome, large areas of leveled SI surfaces were observed. Specifically, such leveled surfaces are favorable for the formation of areal slush flows from a water-saturated snow strip at the boundary with the snow cover upslope. In many cases, this led to an accelerated disappearance of the snow cover on separate areas of the dome, especially on north-facing slopes.

Characteristics of SI on the ice dome

According to the author's measurements, the average thickness of the annual SI layer on the ice dome is 15–16 cm. Depending on the relief of the surface and the presence of crevasses, the thickness of the layer varied from 2 to 24 cm or more. The minimum thickness of SI (about 2 cm) was recorded at the lower side of perpendicular long-term crevasses in the western part of the ice dome. This indicates that the freezing of water entering from upslope areas played an important role in the formation of superimposed ice.

If, during the summer, snow in the upper part of the ice dome does not melt fully, as it happened in 2009–2016, as well as partially in 2017–2019, then SI, which accumulated at the beginning of the ablation season, does not melt under the snow cover. At the beginning of the next ablation season, a new SI layer begins to grow on the SI layer from the previous year. Thus, the thickness of the SI layer is summated. Given an average thickness of annually accumulating SI layer of approximately 15 cm, a maximum thickness of approximately 75 cm accumulated during five years was first observed on the ice dome. Then, the maximum thickness of SI was found to be equal to 145 cm near stake R12 on the eastern slope of the dome in March 2019. In some areas along the periphery of the ice dome, the SI thickness reached 1.5 m, which is indicative of about a decade of its continuous accumulation. The SI thickness of 3 m was recorded near stake R7 in ice crevasse under snow and firn.

Data on the average thickness of the SI layer on the Bellingshausen Ice Dome in different years are provided in Table 1. They indicate that only in 2007–

2009, 2017–2018, and 2020 the average SI layer showed annual growth of up to 16 cm. In other years, the average SI thickness was higher because of the SI accumulation over several years.

To compare, Table 2 shows data on SI for different regions. It can be seen that the predominant SI thickness accumulated during one summer season in different regions is in the interval of 10–20 cm and increases up to 27–35 cm only high in the mountains on the Aktru Glacier, at the boundary of the firn–ice and cold firn zones in conditions of continental climate of the Altai Mountains. On glaciers of the Suntar-Khayata Ridge, in conditions of cold climate, similar thicknesses of seasonal SI were recorded in the ablation zone. Larger SI thickness values obtained for the Kongsvegen Glacier (Spitsbergen) were possibly related to damming of meltwater in the snow cover within separate parts of the glacier.

The density of SI on the ice dome slopes was measured in 10- to 40-cm-long ice cores and reached 0.66–0.91 g/cm^3. Such a wide range of SI densities is apparently connected to the structure of wet snow, the presence or absence of ice interlayers and their thickness, as well as to the number of air bubbles in the ice. Average data from 97 samples showed SI density equal to 0.82 g/cm^3. The obtained average SI density on the Bellingshausen Ice Dome agrees well with data from other glaciers (Table 2): 0.8 g/cm^3 for Kongsvegen Glacier on Spitsbergen [*Brandt et al., 2008*], 0.87 g/cm^3 for Xiao Dongkemadi Glacier on the Tibetan Plateau [*Fujita et al., 1996*], 0.89 g/cm^3 for McCall Glacier in Alaska [*Wakahama et al., 1976*], and 0.85–0.91 g/cm^3 [*Bazhev, 1980*] and 0.86–0.98 g/cm^3 [*Shumskii, 1955*] for various glaciers.

A layer of melting crust appears on the surface of melting SI, which, despite having a firn-like snow structure, differs sharply from it. The snow on the surface of the dome is partly covered by dust because dust concentrates on the surface during melting and subsidence of snow. Areal meltwater flows running from a strip of water-saturated snow wash away all dust from the surface of the exposed SI leaving it absolutely clean. Because of this, the surface of the melting SI (melting crust) has a comparable or even a higher albedo than melting snow and a much higher albedo than that of the strip of water-saturated snow and SI just exposed from snow. The following albedo values were obtained through measurements: melting SI, 0.8–0.9 (the average of 13 measurements is 0.85); melting snow, 0.79–0.89 (the average of 8 measurements is 0.85); water-saturated snow, 0.704–0.723 (the average of 4 measurements is 0.716); exposed and not yet melting SI, 0.62–0.64 (the average of 3 measurements is 0.63). The obtained albedo values are close to data for other glaciers [*Cuffey, Paterson, 2010*].

The melting crust surface of the SI is friable and firn-like; it consists of single firn grains of 1–2 mm and more in diameter. The density of the melting SI (to be more exact, the melting crust on SI) varied from 0.6 to 0.9 g/cm^3 (the average of 46 measurements is 0.767 g/cm^3), i.e., it slightly exceeded the

Table 2. **Data on superimposed ice in different regions**

Region	Glacier	SI thickness, cm/yr	Share of SI in mass balance, %	SI density, g/cm^3	Ice formation zone	Source
Spitsbergen	Kongsvegen	(16 ± 6) to 43	15–33 B_w	0.80	fs	[*Brandt et al., 2008*]
Spitsbergen	Kongsvegen	15–(60 ± 10)	35–100		fs	[*Obleitner, Lehning, 2004*]
Spitsbergen	Central Loven	11–18	10–30 B_w		fs	[*Wadham, Nuttal, 2002*]
Spitsbergen	Central Lovem	15	16–25–37		fs	[*Wright et al., 2005*]
Spitsbergen	Store	27	up to 100		fs	[*Jonsson, Hansson, 1990*]
Spitsbergen	Austfonna		5–100 B_w		fs	[*Dunse, 2011*]
Spitsbergen	Aldegonda	15–20			a	[*Solovyanova, Mavlyudov, 2006*]
Spitsbergen	Eastern Grønfjord	12			a	[*Chernov et al., 2015*]
Severnaya Zemlya	Mushketova	17			fs	[*Bolshiyanov et al., 2016*]
Alaska	McCall	20–30–40	50	0.89	fs	[*Wakahama et al., 1976*]
Alaska	McCall		>40 B_w		fs	[*Rabus, Echelmeyer, 1998*]
Baffin Land, Canada	Beims	16.5			fs	[*Baird, 1952*]
Altai	Aktry	20–35			fs–cf	[*Narozhnyi, 2001*]
Suntar-Khayata	No. 30–34	17.5 (5–30)			a	[*Mavlyudov, Ananicheva, 2016*]
Tibet Plateau	Ksnao Dongkemadi		26–60	0.87	fs	[*Fujita et al., 1996*]
Various regions			up to 80–100	0.85–0.91	fs–cf	[*Bazhev, 1980*]
King George Island	Ekologic	10–15			fs	[*Gonera, Rachlewicz, 1997*]
King George Island	Ekologic	7	up to 20		fs	[*Rachlewicz, 1999*]
Different Regions				0.86–0.89	fs–cf	[*Shumskii, 1955*]

Note: B_w is winter mass balance; ice formation zones: cf – cold firn zone, fs – firn–snow zone, and a – ablation zone.

density of the firn and was slightly less than the density of the SI not subjected to melting. The significant difference in density values of the melting crust on SI depended on the presence and thickness of ice interlayers existing in the snow and firn before the formation of SI.

Specific features of SI melting

The melting of SI begins under a thin layer of snow under the influence of solar radiation. Small inner channels forming a sparse dendritic network of voids are developed in the SI thickness at shallow depths. The density of these channels can reach 5 m per 1 m^2 and more. How exactly are they formed in the SI thickness is not quite clear. It is possible that they develop from air bubbles, which are abundant in the SI. Under the thick layer of snow, channels are not formed; melting inside the ice begins under the influence of solar radiation, when the thickness of the snow becomes less than 0.5–0.6 m. The melting of inner channels that appear in the SI thickness creates unevenness on its surface in the form of shallow dry channels (Fig. 2*f*).

At the first exposure from under the snow, the water permeability of the SI layer is low, and the borehole drilled in it remains completely filled by water. But as soon as the area of the exposed SI widens and a melting crust is formed in its central part, no water remains in the boreholes near the upper boundary of the exposed area of SI, because water is drained through the melting crust. On the contrary, in the boreholes drilled along the lower boundary of the exposed SI area (below the field of exposed glacier ice), the water level stands at the top of the boreholes, because of the absence of drainage channels in the SI thickness.

The layer of SI under the snow cover preserved after the summer season and the adjacent part of exposed SI contribute to the increase in the thickness of the glacier ice. In 2007/08 and 2008/09, the SI melted almost entirely on the Bellingshausen Ice Dome; in 2009/10, it was preserved in some locations the southern and northwestern parts of the dome above 170 m asl. At higher elevations, SI was preserved everywhere. In 2010/11 and 2011/12, it was preserved at elevations above 180 m asl (on average). In 2012/13–2014/15, the SI layer on the dome did not melt out under the preserved snow. Active melting of the SI continued in 2016/17 and 2017/18 because of high summer air temperatures; in 2018/19 the SI melting was reduced because of frequent summertime snowfalls. In summers of 2019/20 and 2020/21, melting of the SI was active (Table 1). According to our estimates, except for cold seasons of 2009/10, 2012/13–2015/16, and 2018/19, when snow was preserved almost on the entire surface of the dome until the end of the ablation season, the melting of the SI reached approximately 9 cm in water equivalent (w.e.) and more. In summers of 2011/12, 2016/17, 2017/18, 2019/20, and 2020/21, the SI layer, which had accumulated over previous years, melted away completely. A comparison of average melting rates of the SI on the dome with the mean summer temperatures recorded at the Bellingshausen weather station (Fig. 3) demonstrated their relatively close relationship with the coefficient of determination $R^2 = 0.66$.

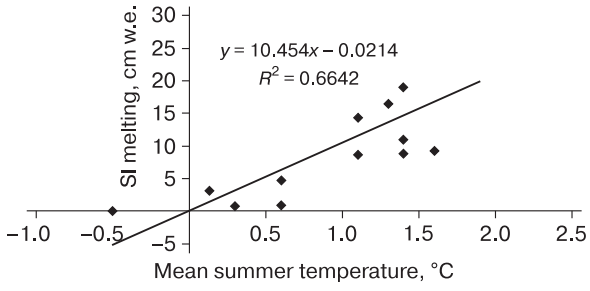

Fig. 3. Averaged melting rate (stake measurements) versus mean air summer temperatures at Bellingshausen weather station in 2007–2021.

Duration of the SI formation at different elevations of the ice dome

The formation of SI on the ice dome most often did not exceed one month. During years with positive mass balance, the growth of SI in the lower part of the dome began in December and ended in January, and sometimes could last throughout the entire summer with varying intensity, as it happened in 2014/15. During years with negative mass balance, the growth of the SI in the lower part of the dome began in November and ended in December. In individual years, certain shifts in the dates of SI growth in dependence

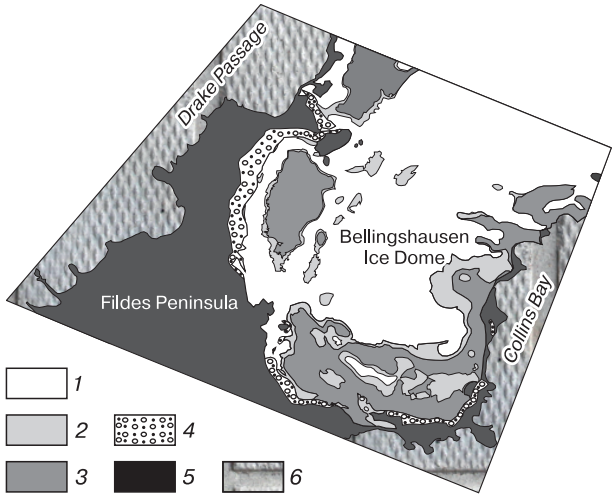

Fig. 4. Distribution of different types of snow–ice formations on the Bellingshausen Ice Dome.

1 – snow, *2* – superimposed ice, *3* – glacier ice, *4* – moraine, *5* – ice-free area, *6* – sea. Composed on the basis of TerraSAR-X radar image from March 12, 2011 (the end of ablation period).

on the height of the dome were recorded. On the top of the dome, the growth of SI during active snow melting, could begin simultaneously with its growth at the lower part of the dome (2014/15 and 2016/17) or 1.5–2.5 weeks later. The end of the SI formation on the top of the dome could take place in 0.5–1.5 months after the end of this process at the lower part of the dome. The duration of the SI formation shortened considerably in summers with positive air temperatures, abundant and frequent rainfalls, and periods with thick fogs. The duration of the SI formation increased in summers with cold weather, solid (snow) precipitation, and blizzards alternating with periods of warm weather.

Distribution of superimposed ice

The greatest extent of SI on the dome was noted in periods with rapid exposure of the SI surface out of the snow cover. Then, the area of the SI distribution decreased (Fig. 4).

The area of SI distribution increased in the years with warm weather after a series of years with a positive mass balance (2016/17, 2017/18, 2019/20). In such cases, the strip of the simultaneously exposed SI was more than 300 m wide because of the melting of SI of considerable thickness accumulated during several years. The largest recorded width of the SI strip (900 m, more than half of the slope of the ice dome) was recorded on March 21, 2012 on the southeastern slope of the ice dome and on December 31, 2019 on the southern slope of the dome.

DISCUSSION

This study, as well as previous research [*Wadham, Nuttal, 2002*], demonstrates that the formation of SI can occur in one step (during the spring) or in two steps (in the autumn at the end of melting on the dome and in the spring). A greater part of the SI thickness forms during the spring stage. In the spring, SI formation occurs everywhere, whereas in autumn it only takes place within the fields of snow, in the course of freezing of snowmelt during autumn (in some cases, also summer) cooling. Below on slope of the snow fields, the freezing of meltwater flowing from them leads to the formation of a congelation ice layer above the glacier ice [*Koreisha, 1991*]. The thickness of the autumn SI depends on the water saturation of the snow higher up the slope and on the degree of cooling at the end of the ablation season. More favorable conditions for the formation of SI are created if rainy weather is abruptly changed by cooling in autumn. In that case, rainwater seeping through the snow joins snowmelt runoff.

In the ablation zone, SI can be seasonal, but it can easily survive for two years (pereletok) or more, if the snow cover on some area or on the entire surface of the ice dome does not melt during the summer season. At negative mass balance on the ice dome, the SI is exposed on the surface as a strip of varying width at the boundary between the glacier ice and snow (Fig. 2*b*, *c*). At even melting of a consistently thick snow cover, vast surfaces of the ice dome can become simultaneously covered by SI. This usually lasts a short time (depending on the weather, from one week and more). After a long period with a positive mass balance, at a large thickness of accumulated SI (75 cm and more), its melting on the surface of the glacier can take a long time. During the summer of 2016/17, melting of the SI in the lower part of the ice dome lasted over 46 days; in the upper part of the dome, it affected only the topmost part of the SI thickness, while its main part remained unchanged. In March 2019, the SI near stake R11 was more than 125 cm in thickness.

As SI characterizes accumulation and its lower boundary corresponds to the equilibrium line of the glacier, the melting of the long-term SI on the slopes of the ice dome complicates the determination of the equilibrium line for the particular year, because it is virtually impossible to separate between annual ice layers within continuous SI thickness. It is possible to determine the equilibrium line elevation only in individual places near measuring stakes and between them. The accumulation of SI over several years can become a reason for the lack of possibility to reliably determine the equilibrium line altitude of the Bellingshausen Ice Dome upon complete melting of the snow cover and exposure of the SI. This is true for all kinds of terrain research and remote sensing, if stake measurements are not conducted. Stake observations are a must on the glaciers and ice domes of the studied Antarctic region, because even studies of SI in pits and boreholes do not allow for accurate identification of the year to which a specific part of the SI layer belongs.

Two types of glacier feeding exist on the ice dome: (a) transformation of nonmelted snow into firn in the firn–ice zone and (b) accumulation of SI at the base part of the snow cover in the infiltration–congelation zone. In the latter case, direct transformation of snow into ice occurs during refreezing of meltwater. In the first case, the formation of glacier ice occurs in several steps. First, snow which has not melted during the summer, transforms into firn containing numerous ice grains, lenses and interlayers, as well as a layer of SI at the snow base. Subsequently, by to inner feeding, the amount of ice in the firn thickness increases, and the growth of SI in the lower part of the firn layer continues. In many cases, it was recorded (near stakes R6, R14, 9N, and IN) that the SI appears within the firn layer and isolates the underlying firn from meltwater. As a result, layers and lenses of firn are preserved inside the ice thickness. It is possible that future radar research of the snow–firn layer in the upper part of the ice dome will indicate how widespread is this phenomenon and what is the

thickness of the suspended SI layer (or layers) in the firn–ice body. In particular, studies of ice cores from the top of the dome in 1992 demonstrated the presence of firn interlayers down to a depth of 7 m below the surface [*Wen et al., 1998*].

Regardless of the sign of mass balance of ice on the dome in general, in recent years, there always have been areas, where SI melted away entirely, and areas, where it continued to accumulate. In years with a positive mass balance, the accumulation of SI took place over a larger part of the dome, and in years with a negative mass balance, it took place only in the areas with preserved snow–firn thickness. During warmer periods, the role of the SI layer as a sink of moisture decreases, whereas during cooling it increases. Currently, the accumulation of SI is the only process of ice formation on the ice dome, because even in the upper part of the dome, the thickness of the accumulating snow and firn is clearly insufficient for their transformation into ice under their own weight.

The process of ice formation on the dome through growth of the SI thickness is typical not only for the present time. In some parts of the glacier (for example, near stakes R5 and FN), after melting of the snow cover and SI, glacier ice with ice crystals of 2–3 mm becomes exposed and quickly transforms into the snowlike mass of melting crust under the impact of solar radiation. This glacier ice was formed from the SI in the past. It differs from the modern SI by the presence of numerous crevasses filled by macrocrystalline ice (which formed during the freezing of water in crevasses) and cryoconite holes of varying sizes, which emerged upon melting of the ice enriched in volcanic ash particles. Such structures do not exist on the surface of modern SI.

If we take the average thickness of SI accumulating on the Bellingshausen Ice Dome over a year equal to 15 cm (or 12.2 cm w.e.) and assume that SI forms under the snow and firn of any thickness, it becomes possible to estimate the portion of SI in the water content of the snow of varying thickness (Fig. 5).

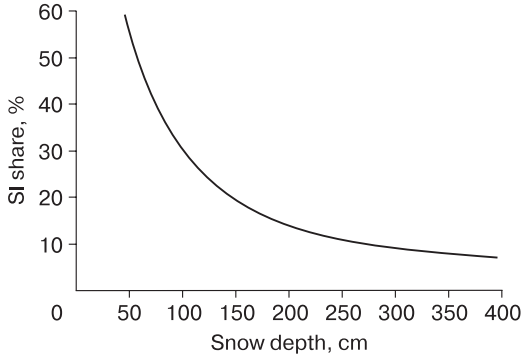

Fig. 5. Dependence of the water content of SI on the snow cover depth.

Annual water equivalent of SI 12.2 cm w.e., snow density 0.5 g/cm^3.

The portion of the SI layer in the winter mass balance on the ice dome depends on the snow thickness and decreases exponentially with an increase in the snow thickness. However, the curve in Fig. 5 is merely theoretical, because at a small snow thickness, such an SI layer is unlikely to form because of warming of the snow thickness by solar radiation. This means that at a small snow thickness, the SI layer should also have a smaller thickness, but its portion in the winter mass balance will be preserved. At an average thickness of annually accumulating snow of about 1.0–1.5 m, the SI layer portion in the winter mass balance can be estimated at 20–30%, which is confirmed by measurements at stakes (Table 1). If average values of snow and ice melting and the thickness of melted away SI measured at stakes on the dome are taken into account, then the portion of melting SI in the summer mass balance on the dome can be estimated. This melted part of the SI does not exceed 20% of the total mass balance; it increases in

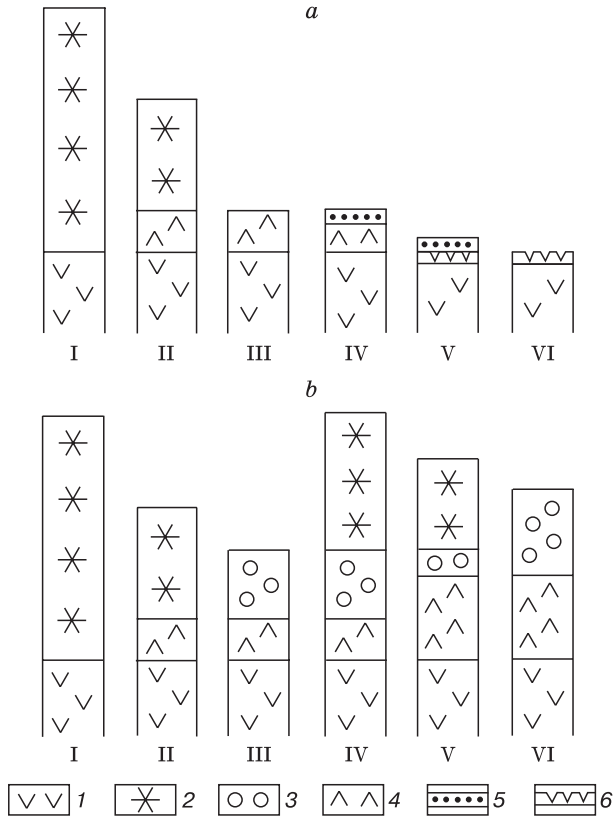

Fig. 6. Mechanisms of formation and changes in the superimposed ice on the Bellingshausen Ice Dome upon (*a*) complete melting and (*b*) long-term accumulation.

1 – glacier ice, *2* – snow, *3* – firn, *4* – SI, *5* – melting crust at the SI surface, *6* – melting crust at the glacier ice surface; (I–VI) sequence of changes.

years with a negative mass balance and decreases in years with a positive mass balance.

Two mechanisms of SI formation and change can be observed on the Bellingshausen Ice Dome: (1) the accumulation of SI at the base of the snow and firn layer and its complete melting after the disappearance of the snow–firn thickness during the ablation season; and (2) the accumulation of SI at the base of the snow and firn layer, its preservation under a layer of nonmelted snow and firn, and the continuing accumulation of a new SI layer over the SI layer of the previous year (Fig. 6). The first mechanism domi-

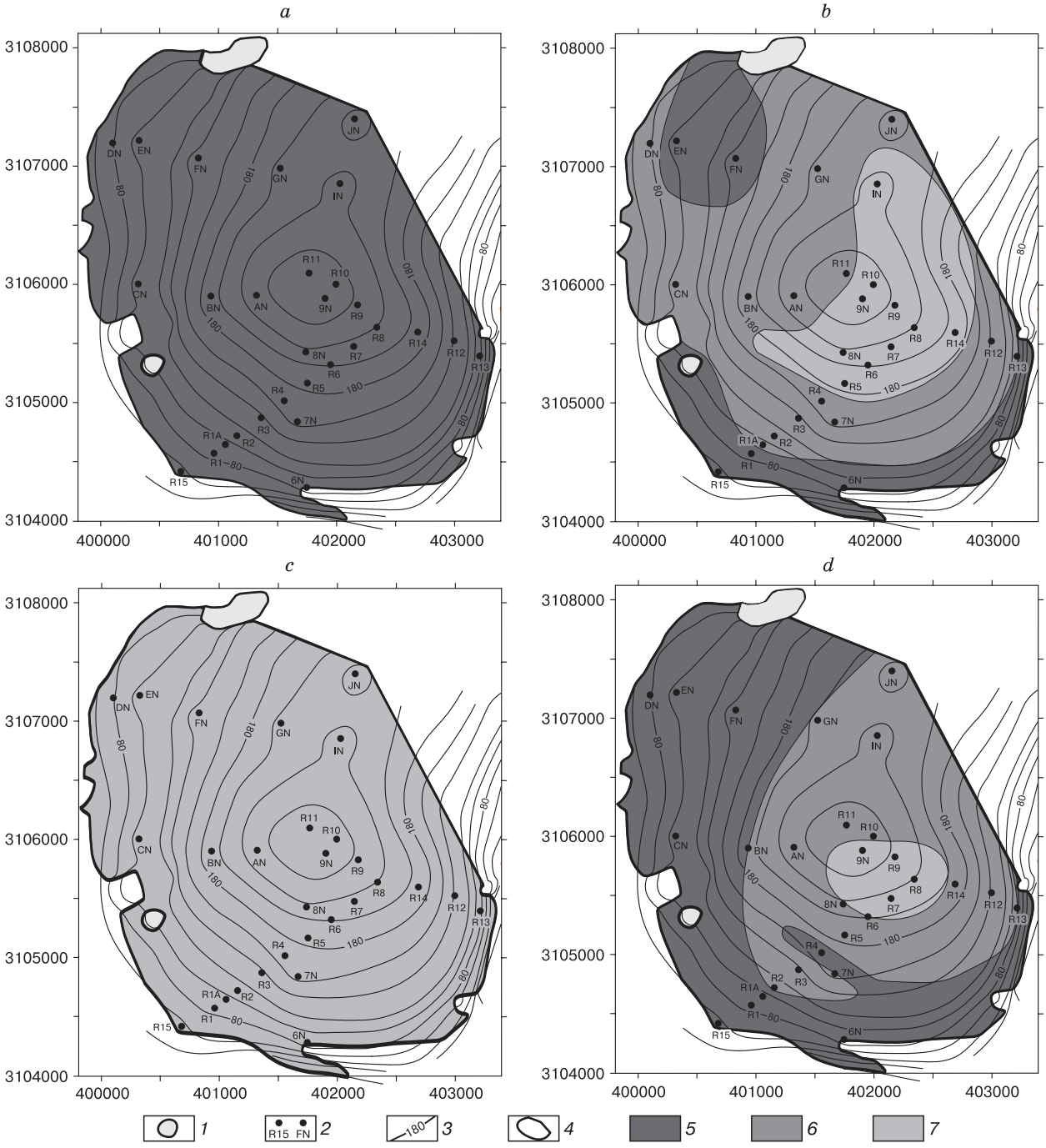

Fig. 7. Distribution of SI fields on the Bellingshausen Ice Dome in different periods: (*a*) 2007–2009, (*b*) 2009–2012, (*c*) 2012–2016, and (*d*) 2016–2021.

1 – nunataks, *2* – stakes and their numbers, *3* – contour lines on the dome surface, *4* – boundaries of the Bellingshausen Ice Dome; *5–7*, zones of SI accumulation (*5* – seasonal, *6* – melting, *7* – long-term).

nates in the periphery of the ice dome, and the second mechanism is observed in the upper part of the dome (Fig. 4).

At the dome surface area of 8.9 km^2 and the average thickness of SI of 15 cm (12.2 cm w.e.), the total volume of SI on the dome at the beginning of the summer can be estimated at $1.34 \cdot 10^6$ m^3, or $1.09 \cdot 10^6$ t. This is approximately equal to the annual increase in the amount of glacier ice (without snow and firn) in water equivalents in years with a positive ice mass balance. During the summer, the amount of SI accumulated in a particular year decreases. The higher the summer air temperature, the lesser the amount of SI preserved toward the end of the ablation season and vice versa. In recent years, during periods with a negative mass balance, approximately 400,000 t of SI have been preserved on the dome annually.

Three zones can be identified on the Bellingshausen Ice Dome: the zone of seasonal SI accumulation (the average thickness is 15 cm, regardless of the time of measurements), the zone of melting SI, and the zone of accumulating SI (Fig. 7).

In the first years of this study, the accumulation of only seasonal SI took place on the ice dome (Fig. 7*a*). After 2009, an area of continuous accumulation of SI with a total thickness of up to 45 cm appeared on the southeastern side of the dome; it was bordered by the transitional area of melting SI of 0–45 cm in thickness (Fig. 7*b*). In 2012–2016, a continuous growth of the SI thickness took place on the whole area of the ice dome, up to 60 cm on the periphery and up to 100 cm near the dome's top (Fig. 7*c*). In 2016–2021, a complete melting of SI took place along the periphery of the dome, where the SI thickness reached 150 cm. In the area of ablation stake R7, in a crevasse, the SI thickness measured in the summer of 2020/21 was up to 300 cm (Fig. 7*d*). Thus, the distribution and thickness of the SI on the dome changed in time and in space. The further accumulation of SI and its distribution within the dome will depend on climate changes.

CONCLUSIONS

Superimposed ice plays the same role in the ice dome's mass balance as nonmelted snow: about 20–30% of the winter balance and up to 20% of the summer balance.

The functioning of SI can be summarized as follows:

(1) Superimposed ice levels the surface of glaciers, which is favorable for the development of flush flows that accelerate the removal of snow from the surface of glaciers. Because of the leveling of the glacier surface by SI, water flows may change the position of their channels in space. Sometimes, meandering former channels of water streams can be seen on the exposed glacier surface. Such channels remain filled with SI for a long time.

(2) Superimposed ice contributes to the transformation of the outer layer of glacier ice under it. The ice of the Bellingshausen Ice Dome is greatly contaminated by volcanic ash particles derived from eruptions of the Deception Volcano. As a result of partial melting and decreasing thickness of SI, the underlying glacier ice becomes subjected to the action of direct solar radiation. First of all, dark ash particles are heated and favor ice melting. Therefore, the surface of glacier ice under SI is often dissected by vertical microchannels containing ash particles on the bottom. Thus, a specific melting crust is formed in the glacier ice; the latter becomes less dense (0.3 g/cm^3 and less) and acquires openwork structure because of the presence of a large number of voids. Similar phenomenon was described by the author for Spitsbergen glaciers [*Mavlyudov, 2008*]. Rapid melting of such ice after the disappearance of SI contributes to the leveling of the surface of glacier ice.

(3) Superimposed ice accelerates the transformation of snow and firn into ice without considerable growth in their thickness.

(4) The forming SI suspends snow melting; despite settling of the snow surface, the water content of the snow remains relatively stable in the period of SI formation. If this SI becomes exposed to the surface, its melting requires more energy than the melting of snow, which was indicated in [*Koreisha, 1991*].

(5) In contrast to many other areas, the strip of exposed SI on the Bellingshausen Ice Dome has a significant width (tens and hundreds of meters) at the end of the ablation season, which is related to the simultaneous melting of snow and firn over large areas and to the long-term accumulation of SI.

(6) Regardless of the density of SI on the Bellingshausen Ice Dome, the melting crust on its surface represents a firn-like friable mass of rounded ice grains of 1–3 mm in diameter, which can serve as evidence of the mainly infiltration origin of the SI. The role of congelation in the SI formation is less significant.

The formation of SI on glaciers plays an important role in slowing the response of the glacier mass balance to climate change [*Wang et al., 2015*]. With climate warming, which is observed in many regions, the amount of forming and preserved SI should decrease; SI is unlikely to influence the mass balance of glaciers more in the future than it currently does. It is probable that the role of SI in glacier mass balance should decrease with further warming. However, it may also increase upon climate cooling, when the ice temperature under the snow becomes lower, whereas summer melting of the accumulated snow does not change much. This is possible upon winter cooling and preservation of summer temperatures. At the same time, as SI is a transformed part of the snow

cover, the change in its share in the snow cover upon climate changes should be reflected in the glacier mass balance value. An additional possibility of slower snow melting in the areas of SI accumulation can be related to the formation of SI not only from local meltwater but also from dammed meltwater flowing down the slope from upslope positions. The redistribution of meltwater on slopes can lead to some increase in the SI thickness and retard snow melting. The particular patterns of meltwater flows depend on the local features of the relief of the glacier rather than on climate changes.

It is believed that SI formation decreases runoff from glaciers as compared with that under conditions without refreezing [*Wang et al., 2015*]. Indeed, in polar and alpine regions, SI thickness increases, while its decrease in observed in the middle latitudes. This means that the amount of water stored in SI decreases as we move away from polar and alpine regions. At the same time, no significant amounts of SI are formed on warm glaciers, where the role of SI in the regulation of water discharge from the glaciers is relatively small.

Annually accumulating SI layer (of any thickness) preserved on the dome at the end of summer is indicative of a positive ice mass balance, while the complete melting of SI layer attests to negative mass balance at each particular point of the glacier.

Previous researchers do not note the exposure of SI to the surface of the Bellingshausen Ice Dome. Nonetheless, there is no doubt that SI formed and was exposed to the surface in the past, as well as at present. In 1968–1970, the equilibrium line altitude of the ice dome was at 120–145 m asl [*Zamoruev, 1972*], so the strip of SI exposed after melting of snow and firn could exist along this line. Undoubtedly, in the upper part of the dome, where a warm firn zone was found, SI, together with the innerfeeding partially or completely blocked water discharge from the upper zone.

Thus, the origin, current state, and dynamics of SI on the Bellingshausen Ice Dome are considered in this article. It is demonstrated that the SI layer in the lower part of the snow cover is distributed everywhere throughout the dome; in some parts of the dome, it has a seasonal character and melts away by the end of summer. The SI layer is preserved under the snow cover and merges together with the SI formed in the previous year(s). At the average annual accumulation of SI of about 15 cm, the presence of areas, where the SI layer has a thickness of 145–150 cm and even 300 cm in some places, confirms its long-term accumulation. The presence of areas with a long-term accumulation of SI creates a problem for the exact determination of the equilibrium line altitude in particular positions on the dome. In fact, it cannot be determined by field or remote sensing methods, except for regular measurements at ablation stakes.

Acknowledgments. *The author extends his gratitude to directorship of the Institute of Geography, Russian Academy of Sciences, and to the Russian Antarctic Expedition for the opportunity to conduct long-term monitoring of glaciers on King George (Waterloo) Island in Antarctica.*

Funding. This study was performed within the framework of state assignments of the Institute of Geography, Russian Academy of Sciences no. AAAA-A19-119022190172-5 (FMGE-2019-0004) "Glaciation and Associated Natural Processes during Climate Change".

References

Baird P.D., 1952. The glaciological studies of the Baffin Island Expedition, 1950. Part I: Method of nourishment of the Barnes Ice Cap. *J. Glaciol.* **2** (11), 2–9, 17–19.

Bazhev A.B., 1973. The role of infiltration feeding in glacier mass balance and the methods of its measurements. *Mater. Glyatsiologich. Issled.* **21**, 219–231 (in Russian).

Bazhev A.B., 1980. Methods for determining infiltration feeding of glaciers. *Mater. Glyatsiologich. Issled.* **39**, 73–81 (in Russian).

Bolshiyanov D.Y., Sokolov V.T., Yozhikov I.S. et al., 2016. Alimentation conditions and variability of glaciers of the Severnaya Zemlya Archipelago according to observations in 2014–2015. *Led i Sneg* **56** (3), 358–368 (in Russian).

Brandt O., Kohler J., Lüthje M., 2008. Spatial mapping of multiyear superimposed ice on the glacier Kongsvegen. *Svalbard. J. Glaciol.* **54** (184), 73–80.

Chernov R.A., Vasilyeva T.V., Kudikov A.V., 2015. Temperature regime of the upper layer of the Eastern Grönfjordbreen Glacier (West Spitsbergen). *Led i Sneg* **55** (3), 38–46 (in Russian).

Cogley J.G., Hock R., Rasmussen L.A. et al., 2011. *Glossary of Glacier Mass Balance and Related Terms.* IHP-VII Technical Documents in Hydrology, No. 86, IACS Contribution No. 2, UNESCO-IHP, Paris, 115 pp.

Cuffey K.M., Paterson W.S.B., 2010. *The Physics of Glaciers.* Fourth ed. Amsterdam, Academic Press, 704 pp.

Dunse T., 2011. Glacier Dynamics and Subsurface Classification of Austfonna, Svalbard: Inferences from Observations and Modeling. PhD Diss., University of Oslo, Oslo, Norway, 175 pp.

Fujita K., Seko K., Ageta Y. et al., 1996. Superimposed ice in glacier mass balance on the Tibetan Plateau. *J. Glaciol.* **42** (142), 454–460.

Gardiner M., Ellis-Evans J.C., Anderson M.G., Tranter M., 1998. Snowmelt modelling on Signy Island, South Orkney Islands. *Ann. Glaciol.* **26**, 161–166.

Gonera P., Rachlewicz G., 1997. Snow cover in the vicinity of Arctowski Station, King George Island, in winter 1991. *Polish Polar Res.* **18** (1), 3–14.

Jiankang H., Zichu X., Fengnian D., Wanchang Z., 1999. Volcanic eruptions recorded in an ice core from Collins Ice Cap, King George Island, Antarctica. *Ann. Glaciol.* **29**, 121–125.

Jonsson S., Hansson M., 1990. Identification of annual layers in superimposed ice from Storöyjokelen in northeastern Svalbard. *Geografiska Annaler* **72A**, 41–54.

Koreisha M.M., 1991. *Glaciation of the Verkhoyansk–Kolyma region. Results of the IGY Investigation.* Moscow, Interagency Geophysical Committee, 143 pp. (in Russian).

Kotlyakov V.M. (ed.), 1984. *Glaciological Glossary*. Leningrad, Gidrometeoizdat, 528 pp. (in Russian).

Mavlyudov B.R., 2008. Melting crust on Aldegonda Glacier, Spitsbergen. *Arktika i Antarktika* **40** (6), 33–54 (in Russian).

Mavlyudov B.R., 2016. Bellingshausen Dome, Antarctic. *Geography of Polar Regions. Problemy geografii* **142**, Moscow, Kodeks, pp. 629–648 (in Russian).

Mavlyudov B.R., Ananicheva M.D., 2016. Glacier dynamics in the northern massif of the Suntar-Khayata Mountains: modern conditions and dynamics from the end of the 1950s. *Led i Sneg* **56**(3), 345–357 (in Russian).

Narozhnyi Yu.K., 2001. Zones of ice formation and specificity of the structure of snow–firn deposits on Aktru glaciers. *Vestn. Tomsk. Gos. Univ.* **274**, 40–50 (in Russian).

Obleitner F., Lehning M., 2004. Measurement and simulation of snow and superimposed ice at the Kongsvegen glacier, Svalbard (Spitzbergen). *J. Geophys. Res.* **109**, D04106.

Rabus B.T., Echelmeyer K.A., 1998. The mass balance of McCall Glacier, Brooks Range, Alaska, USA; its regional relevance and implications for climate change in the Arctic. *J. Glaciol.* **44** (147), 333–351.

Rachlewicz G., 1999. Glacial relief and deposits of the western coast of Admiralty Bay, King George Island, South Shetland Islands. *Polish Polar Res.* **20** (2), 89–130.

Shumskii P.A., 1955. *Basics of Structural Ice Studies.* Moscow, Izd. Akad. Nauk SSSR, 492 pp. (in Russian).

Solovyanova I.Yu., Mavlyudov B.R., 2006. Studies of superimposed ice on glaciers of Spitsbergen. In: *Multiple Investigation of Spitsbergen Nature*. Apatity, Kola Sci. Center, Russian Acad. Sci., iss. 6, pp. 279–290 (in Russian).

URL: www.aari.aq (last visited: December 15, 2021).

Ushnurtsev S.N., Dyurgerov M.B., Xie Zichu, 1995. Role of superimposed ice in mass exchange of Tien-Shan glaciers. In: *Glaciation of Tien-Shan*. Moscow, pp. 114–120 (in Russian).

Wadham J.L., Nuttal A.-M., 2002. Multiphase formation of superimposed ice during a mass-balance year at maritime high-Arctic glacier. *J. Glaciol.* **48** (163), 545–551.

Wakahama G., Kuroiwa D., Hascmi T., Benson C.S., 1976. Field observations and experimental and theoretical studies on the superimposed ice of McCall Glacier, Alaska. *J. Glaciol.* **16** (74), 135–149.

Wang C., Cheng B., Wang K., Gerland S., Pavlova O., 2015. Modelling snow ice and superimposed ice on landfast sea ice in Kongsfjorden, Svalbard. *Polar Res.* **34**, 20828. DOI: 10.3402/polar.v34.20828.

Wen J., Kang J., Xie Z. et al., 1998. Glaciological studies on the King George Island ice cap, South Shetland Islands, Antarctica. *Ann. Glaciol.* **27**, 105–109.

Wright A., Wadham J., Siegert M. et al., 2005. Modelling the impact of superimposed ice on the mass balance of an Arctic glacier under scenarios of future climate change. *Ann. Glaciol.* **42**, 277–283.

Wright A.P., Wadham J.L., Siegert M.J. et al., 2007. Modeling the refreezing of meltwater as superimposed ice on a high Arctic glacier: A comparison of approaches. *J. Geophys. Res.* **112**, p. F04016.

Zamoruev V.V., 1972. Results of glaciological observations on Bellingshausen station in 1968. *Tr. Sovetsk. Antarktich. Ekspeditsii* **55**, 135–144 (in Russian).

Received November 22, 2021
Revised February 18, 2022
Accepted September 13, 2022

Translated by M.A. Korkka